用√符号选择一类	
教　学	
科　研	√
编号（由专家组填写）	

第十一届全国高校物理实验教学研讨会
本科学生物理实验论文评比表

学生姓名：　　　　　瞿荧飞　　　　　

申报学校：　　　南京信息工程大学　　　

联系方式：电话：　　　15189827172　　　

　　　　　QQ：　　　1807451228　　　

　　　　　E-mail：　jjczquyingfei@126.com　

填表日期：　2020 年 5 月 3 日

全国高校物理实验教学研讨会组委会制

二〇二〇年一月

	姓名	瞿荧飞	性别	女	出生年月	1998 年 3 月
学生作者及发表有关物理实验论文情况	学校名称	南京信息工程大学				
	入学时间	2016		毕业时间		2020
	学　号	20161388032				

（注：论文的第一作者必须为大学本科生，且其论文研究工作是在本科生阶段完成的，到现场答辩的为该论文的学生作者之一。）

论文作者情况（按发表论文作者顺序列出）：

姓名	身份	单位	作用/贡献
瞿荧飞	学生	南京信息工程大学	实验、分析数据、写论文
张启航	学生	南京信息工程大学	数据审核、修改论文
尹文怡	学生	南京信息工程大学	数据审核
胡雨辰	学生	南京信息工程大学	部分作图
刘玉柱	导师	南京信息工程大学	指导老师

简要介绍（研究背景、问题、方法、创新点、学术及应用价值和引用情况等）：

　　研究背景：空气是人类生存的宝贵资源，其破坏是一个不可逆转的过程。因此，空气污染越来越受到重视。而现代的生产生活会产生大量的重金属污染物，这些重金属元素被排放到空气中会极大地污染空气环境，也严重威胁着人类的健康。其中的铅元素和锰元素的危害尤其大。

　　问题：根据空气污染的范围来看它有广域和局域之分，广域的颗粒物重金属污染主要是由工业生产和汽车尾气排放引起的，而局域空气污染主要来源于我们的日常生活，比如说蚊香、农药这类驱虫剂的使用，秸秆的燃烧及烟花爆竹的燃放等。所有这些行为都会对环境造成很大的破坏。近年来，广域大气污染已经引起了人们的高度重视，但是针对局域大气污染的研究还比较少。传统的污染物监测技术皆存在价格昂贵、过程复杂、检测周期长、检测元素单一等弊端，无法对大气中重金属元素进行实时在线的探测和分析。

　　方法：利用激光诱导击穿光谱技术，直接对蚊香燃烧的烟雾、人类的呼吸和周围环

境进行实时原位探测，使用光谱仪采集得到相应的光谱图，并通过高纯度锰块和铅块校正比对确定光谱图中的锰和铅元素的特征谱线。并参考相关文献和数据库，对其他的重金属元素或特征离子进行分析。在此基础上对重金属元素锰和铅的浓度进行半定量的分析，从而证实了利用激光诱导击穿光谱技术对局域大气污染实时原位探测的可行性。

创新点： 利用激光诱导击穿光谱技术，省去了复杂的样品预处理过程，以燃烧的蚊香烟为例，原位实时探测和分析局域空气污染，对其中存在的多种重金属元素实现了快速而高效的检测，可以为局域大气污染的保护提供一定的参照意义。

技术难点： 激光诱导击穿光谱击穿技术光学平台的搭建和优化，数据的采集和校准方面，需要不断的重复和更进。

学术及应用价值： 在大气污染的监测和控制方面有一定的学术参照意义，为采用激光诱导击穿光谱技术对环境污染 (物质成分)进行快速在线检测和分析的可行性提供了技术支持。

指导教师姓名	刘玉柱	职称	教授/博导

对学生发表论文评语及论文情况说明：

指导教师评语

　　瞿荧飞同学在我的指导下积极认真学习激光诱导击穿光谱技术，并开展大气污染研究。多次实验中，统计和分析了大量的实验数据，通过激光诱导击穿光谱击穿技术光学平台的搭建以及多次的重复实验，数据校准，使得采集数据真实可靠，分析充分透彻。其中大部分的工作均由瞿荧飞同学独立完成。
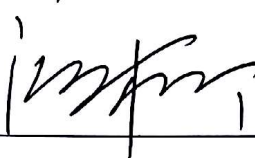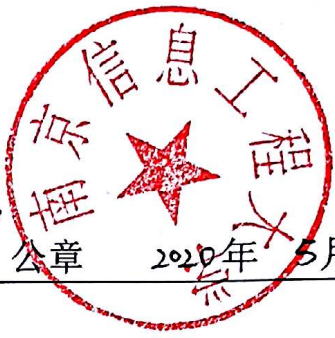
　　在本研究中，瞿荧飞同学利用激光诱导击穿光谱击穿技术，对局域空气污染进行了实时在线的分析和研究，思路清晰，针对相关特征元素分析，数据充分，分析透彻，对局域大气环境的保护具有重要的参照意义，课题研究方案合理可行，有较好的创新性。验证了其用于大气重金属元素分析的可行性，为监测大气污染提供了实验依据和数据参考。

指导教师（签名）：[签名] 　　2020年5月6日

学校推荐意见	同意推荐 负责人（签名）：　　　　　公章　2020年　5月 7日
大会学术组专家意见	 专家组组长（签名）：　　　　　　　年　月　日
评比结果	 理事长（签名）　　　　　　　年　月　日

Real-time in situ detection of the local air pollution with laser-induced breakdown spectroscopy

YINGFEI QU,[1,2] **QIHANG ZHANG,**[1,2] **WENYI YIN,**[1,2] **YUCHEN HU,**[1,2] **AND YUZHU LIU**[1,2,*]

[1]*Jiangsu Key Laboratory for Optoelectronic Detection of Atmosphere and Ocean, Nanjing University of Information Science & Technology, Nanjing 210044, China*
[2]*Jiangsu Collaborative Innovation Center on Atmospheric Environment and Equipment Technology (CICAEET), Nanjing 210044, China*
*yuzhu.liu@gmail.com

Abstract: The smoke of burning mosquito-repellent incense was taken as an example for the local air pollution to be detected and analyzed in situ and in real time. And the spectra of the ambient air, human breathing, and smoke were detected in situ with the LIBS technique. There are some additional spectral lines being found in human breathing, such as the C, H_β line, and the CN molecular bands. Some characteristic peaks of the elements Fe, Ca, Ti, Sr, and Cr have been observed in the smoke. Moreover, the vibrational and rotational temperature of the CN molecule were calculated. The mosquito-repellent incense was dipped into the solutions containing Mn and Pb to simulate heavy metal pollution in the atmosphere.

1. Introduction

Air is a precious resource for human survival, and its destruction is an irreversible process. Therefore, more and more attention has been paid to air pollution. According to the research, atmospheric particulate matter is the main pollutant affecting air quality, among which there are many heavy metals that harmful to human health [1–3]. Based on the scope of air pollution, the wide-area pollution of atmospheric particulates is mainly caused by industrial production and vehicle exhaust emissions [4,5], while the local air pollution mainly comes from our daily life, such as the use of mosquito-repellent incense, pesticide and other insect repellents, burning of straw and discharge of fireworks [6–8]. All these behaviors will cause great damage to the environment.

There are a lot of heavy metal elements in atmospheric particulate matter, among which manganese and lead are two typical elements that do great harm to human beings. Although manganese is an essential trace element we need, excessive manganese can lead to neurological disorders in the brain and irreversible damage to the central nervous system [9]. Lead, which has a strong potential toxicity to many tissues and can cause cancer, has been listed as a strong pollutant [10].

In recent years, wide-area air pollution has won much attention [11–13], but there are few studies on local air pollution. Conventional detection methods for elements include atomic absorption spectrometry (AAS), inductively coupled plasma mass spectrometry (ICP-MS) and so on [14,15]. However, these techniques are not suitable for rapid elemental analysis due to the complex sample pretreatment. Laser induced breakdown spectroscopy (LIBS) is a new technique for the analysis of material composition based on the atomic or molecular spectra in laser-induced plasma [16]. LIBS technique has the advantages of simultaneous multi-element analysis, fast and real-time detection, and small sample loss [17–19], so it has been widely used in different fields [20–22].

LIBS was applied in the experiment, which is one of the important and convenient techniques to analyze the composition of substances. Although LIBS has been applied in

various gas-mixtures and aerosol studies, there is no work reported particularly on attention of the real-time and in situ detection of local air pollution, to our best knowledge. As we know, local air compositions can be easily changed even by the breathing of human. However, the monitoring of human breathing has never been addressed in situ via LIBS technique as well. In this paper, the spectra of human breathing and the ambient air were compared and discussed. What's more, the smoke of burning mosquito-repellent incense was taken as the example for the detection and analysis of the local air pollution in situ and in real time. The mosquito-repellent incense was also dipped in the solution containing Mn and Pb to have a semiquantitative analysis on the atmospheric pollution of heavy metals.

2. Experiment

2.1 Experimental setup

The schematic diagram of LIBS experiment is shown in Fig. 1. All the samples are irradiated by the Q-switched Nd:YAG laser with a fundamental wavelength of 1064 nm and the maximum energy of 680 mJ in a single laser pulse. To increase the stability of signals and improve the quality of image, laser beam used in the experiment was about 290 mJ/pulse with 8 ns duration at a frequency of 10 Hz. The detection of the smoke is challenging. Optical optimization for the laser beam is required. The setting of pulse energy in this experiment is also important. The employed pulse energy is approximately 290 mJ/pulse to achieve the most ideal experimental results. Meanwhile, the delay for the spectrometer is chosen to 6 μs for the best timing setting for this measurement, to detect both the CN molecular spectroscopy (for CO_2 gas in smoke) as well as the atomic spectroscopy (for particulate matter in smoke). The laser been was focused by 15 cm focal length lens onto the ambient air, smoke and other samples. And then a focal spot diameter of about 100 μm would be formed on the surface of the samples, radiating the plasma. The collector could detect the emission signals and transmit them to the spectrometer system to record spectra on the computer via optical fibers. The detection range of spectra is 236—773 nm, and the resolution is about 0.1 nm. Fifty measured spectra were averaged to obtain better signal-to-noise ratio.
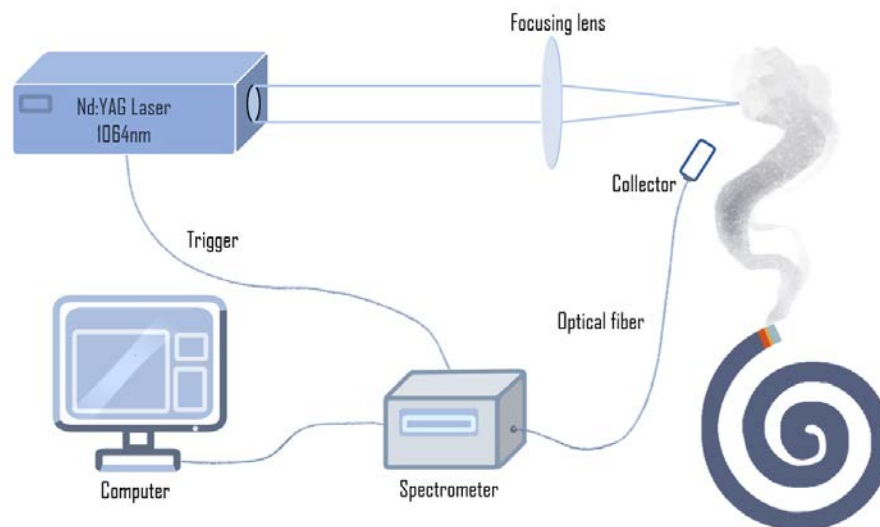

Fig. 1. Schematic diagram of experimental setup.

2.2 Sample preparation

The mosquito-repellent incense analyzed in the experiment is purchased in the supermarket. In order to study the heavy metal pollution in the air, two of the most representative elements,

manganese and lead, were selected in the experiment. Four solutions were prepared and they are two kinds of solutions with different quantity of $Mn(NO_3)_2$ and $(CH_3COO)_2 Pb \cdot 3H_2O$. The high and low concentration of solution $Mn(NO_3)_2$ is 50.0% and 12.5%, respectively. And the high and low concentration of solution $(CH_3COO)_2 Pb \cdot 3H_2O$ is 1.78% and 0.46%, respectively. The mosquito-repellent incense was dipped into the solutions respectively for 15 minutes. And then the samples were dried in the drying oven. Therefore, the water in the mosquito-repellent incense evaporated, and the element Mn and Pb were retained. And the semiquantitative analysis on the heavy metals in the smoke could be carried out.

3. Results and discussion

3.1 Real-time detection of the air and human breathing

In order to have a good analysis of local atmospheric pollution and make it clear, we first obtained the spectrum of the air with LIBS, which is shown in Fig. 2. The characteristic spectral lines of air are mainly distributed in the range of 550 nm through 750 nm. It is well known that the main components of air are nitrogen and oxygen, which are consistent with the characteristic peaks of the spectrum we detected. Since there was some water vapor in the ambient air, the atomic line of hydrogen was also observed at about 656 nm.
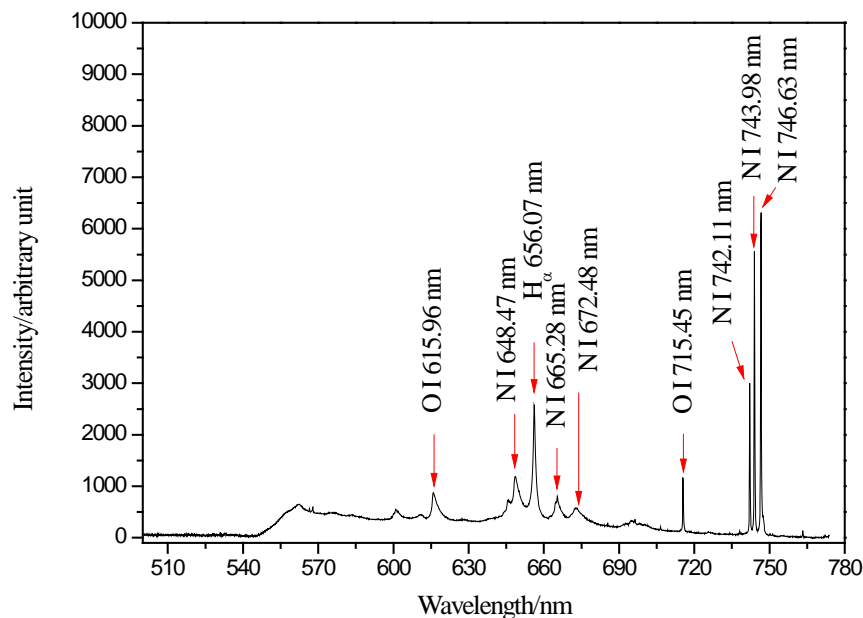

Fig. 2. The spectrum of air ranged from 500nm to 780nm.

After that, human breathing was simulated and the spectrum was recorded, which is compared with the air, as shown in Fig. 3. It can be found that there are some additional spectral lines in the spectrum of human breathing. Referring to the NIST database [23] and some studies [24,25], they were identified as the C I, H_β line and the CN molecular bands, which can be seen more clearly in Fig. 4. This is because human breathing contains carbon dioxide and water vapor. However, hydrogen (H_β) has a weak intensity and it may due to the little content of water vapor.
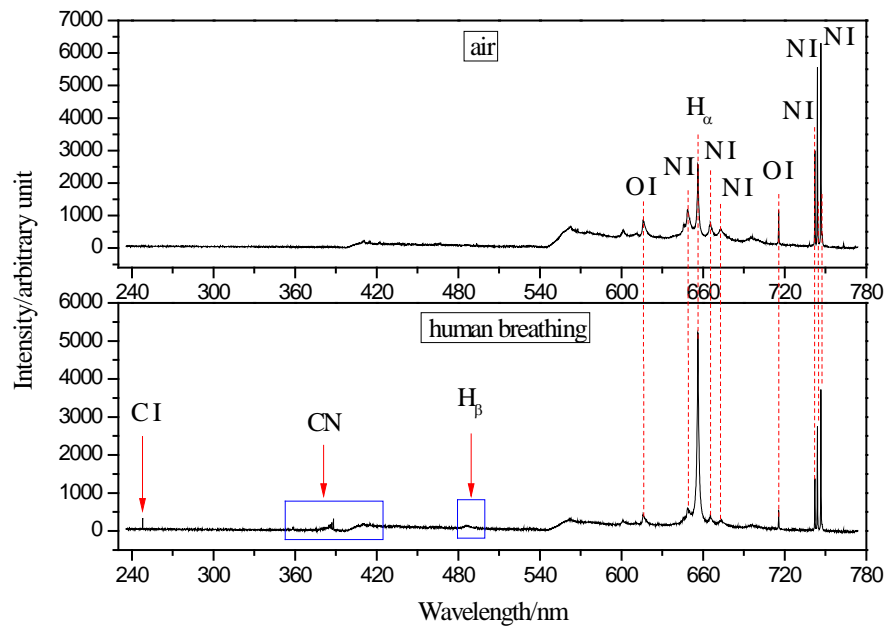
Fig. 3. The spectra of air and human breathing.

The molecular emissions of CN are distributed in the ranges of 355—360 nm, 384—389 nm and 413—422 nm, which correspond to the sequences of $\Delta = +1$, $\Delta = 0$ and $\Delta = -1$, respectively. The results are in good agreement with the previous study of CN bands [26]. However, the sequence of $\Delta = -1$ can't be observed clearly. Since there is no CN in human breathing and air, it is deduced that two reactions may proceed and lead to the formation of CN [27]:

$$C + N \rightarrow CN. \tag{1}$$

$$C + N_2 \rightarrow CN + N. \tag{2}$$

The laser pulse dissociates the N_2 in air and the CO_2 in human breathing, and then the nitrogen and carbon plasma appear. They may recombine to form CN molecule or the atomic carbon would react directly with N_2. What's more, it can be found in the Fig. 3 that the relative intensity of the element N in human breathing decreases, which can also be considered as the evidence that nitrogen in the air participates in reactions.
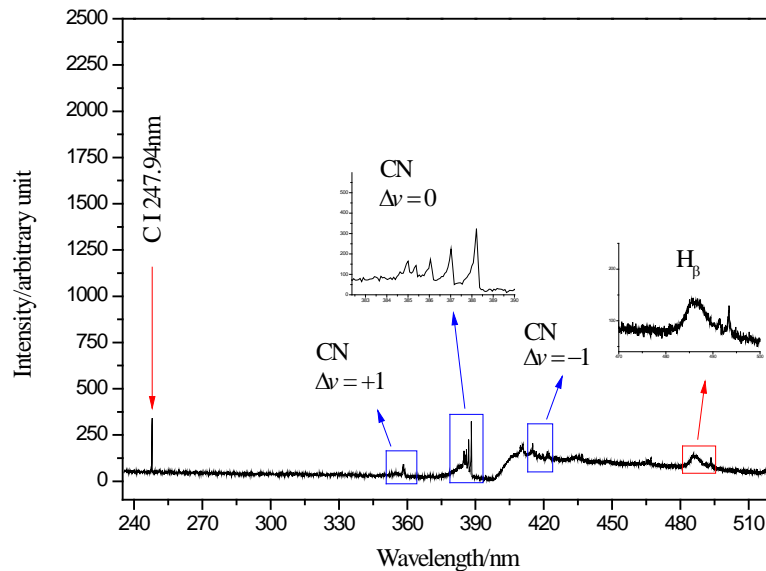
Fig. 4. The spectrum of human breathing ranged from 235 to 520nm.

3.2 Real-time detection of the smoke from burning mosquito-repellent incense

The combustion of mosquito-repellent incense was taken as an example to analyze the local atmospheric pollution, and the smoke of the burning mosquito-repellent incense was detected in situ. In the experiment, the ambient environment was kept free from the unstable air flow. The hot air would generate when the mosquito-repellent incense was lit and it could raise to form a stable channel, from which the smoke could rise continuously. The smoke was captured by igniting the mosquito-repellent incense (without open flames), and it was enclosed by immersing the burning mosquito-repellent incense into water. As depicted in Fig. 5, some metal elements have been identified in the spectra of smoke, such as Mg, Fe, Ca, Ti. Also, it can be found that there are also some toxic elements in the smoke, such as Sr, Cr and Cd [28–30], and somehow the use of mosquito-repellent incense is possibly potential for the pollution to the local atmosphere.

Since the spectra were obtained in the air atmosphere, it is reasonable to observe the spectral lines of nitrogen, oxygen and hydrogen (H_α). In addition, the atomic line of H_β and CN molecular bands are also detected, which do not appear in the spectrum of air. Therefore, it can be speculated that there should be elements such as carbon and hydrogen in the mosquito-repellent incense. A component called meperfluthrin ($C_{17}H_{16}Cl_2F_4O_3$) have been found in the ingredient list of the sample we used. It has great lethality to mosquito and fly, and widely exist in mosquito-repellent incense or pesticides as the additive. The carbon and hydrogen in meperfluthrin may react with nitrogen or oxygen in air to form CN and H_2O. The characteristic spectral line of element fluorine [31] is around 685.6 nm, which was also observed in the experiment, as shown in Fig. 5(c). However, the characteristic line of chlorine is about 837.6 nm [32], which is out of the detection scope for this measurement.
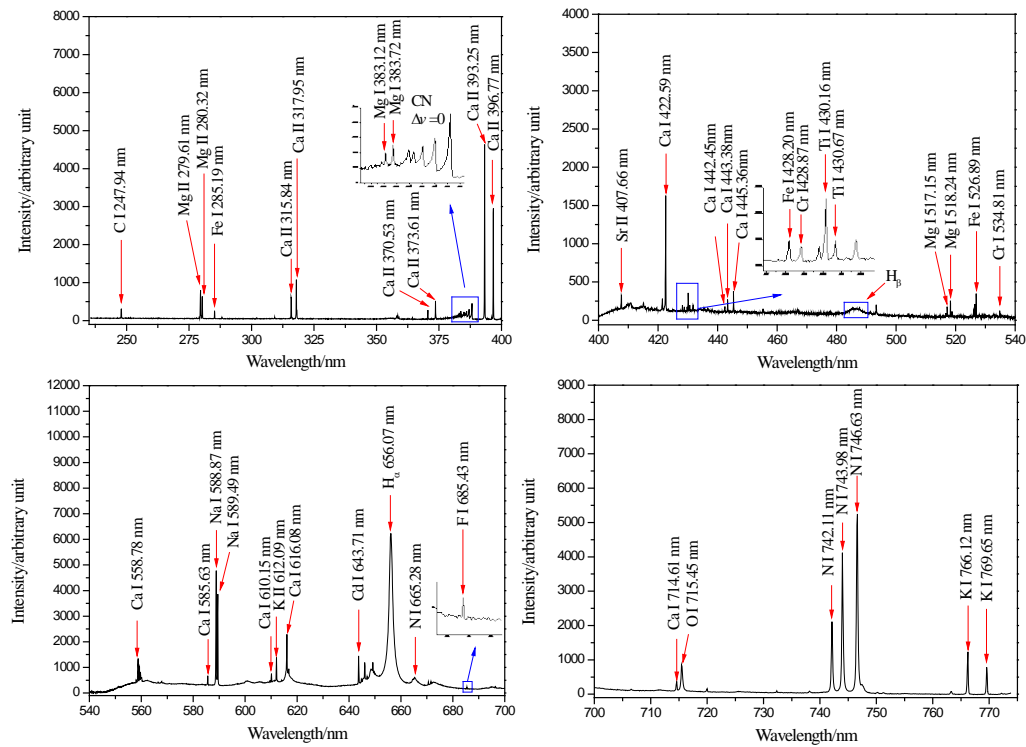
Fig. 5. The spectrum of the smoke.

It should be noted that the carbon from the CN molecule could come from the human breathing, the air or the smoke. However, in the experiment of the naturally occurring in the air, the CN molecular bands were not observed clearly (Fig. 3). It could be reasonably explained by the factor that CO_2 in natural air is too rare to be detected. While when the human breathing (Fig. 4) and the burning mosquito-repellent incense (Fig. 5(a)) occur, the CN molecular spectrum as well as the carbon atomic line (247.94 nm) are clearly observed. Therefore, it is inferred that the carbon of the CN is likely to come from the CO_2 generating from the human breathing and the smoke with higher concentration.

Temperature is one of the most important thermodynamic parameters of molecular radiation. The measurement of the temperature is significant for studying the transitions of molecules and their chemical reactions. Molecular emissions of CN ($B^2\Sigma^+ - X^2\Sigma^+$ band system) have been found in both spectra of human breathing and smoke, of which the $\Delta = +1$ and $\Delta = 0$ sequences can be identified clearly. In the experiment, LIFBASE [33], a spectrum simulation software developed for diatomic molecules and ions, was used to fit the spectral data of the two vibration bands. Baseline and wavelength shift are common phenomena in LIBS technique, and the corrections were done before the simulation to have a more accurate result. In LIFBASE software, the temperature of vibration and rotation were kept adjusting to minimize the mean square error between the results of simulation experiment. The comparison between the two results is shown in Fig. 6, and it can be seen that they are in good agreement. Therefore, the vibrational temperature of CN molecule in human breathing and smoke can be estimated to be 8200 K and 7900 K respectively, and the rotational temperature to be 7600 K and 7000 K respectively. Moreover, the vibrational level populations of CN molecule in $X^2\Sigma^+$ state (v") in the rotational temperature at 7000 K for human breathing and 7600 K for smoke were obtained, as shown in Table 1.

3.3 Semiquantitative analysis of the smoke containing heavy metals

The results demonstrate it is feasible to detect atmospheric particulate matter in situ by applying LIBS technique. With the development of industry, heavy metal pollution in the atmosphere is becoming more and more serious. In order to simulate this, the mosquito-repellent incense was dipped into the solutions containing Mn and Pb element respectively. The excessive intake of manganese will paralyze the central nervous system while lead has been listed in the range of strong pollutants and has strong potential toxicity to the tissues. Hence the two typical elements were selected to have the analysis of heavy metal pollution.

Table 1. The CN molecule vibrational level populations in $X^2\Sigma^+$state

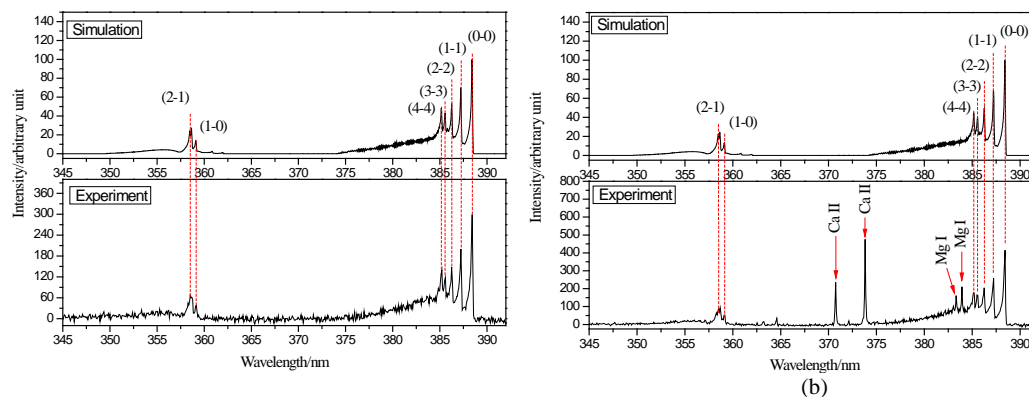| $T_r = 7000K$		$T_r = 7600K$	
$X^2\Sigma^+$ (v")	Vib. Populations	$X^2\Sigma^+$ (v")	Vib. Populations
v" = 0	0.323573	v" = 0	0.315075
v" = 1	0.219789	v" = 1	0.217066
v" = 2	0.150388	v" = 2	0.150601
v" = 3	0.103699	v" = 3	0.105268
v" = 4	0.072094	v" = 4	0.074164
v" = 5	0.050560	v" = 5	0.052691
v" = 6	0.035788	v" = 6	0.037772
v" = 7	0.025630	v" = 7	0.027383
v" = 8	0.018479	v" = 8	0.019980

Fig. 6. The results of simulation and experiment about CN in the human breathing (a) and smoke (b).

The mosquito-repellent incense was lit after drying and then the spectra of smoke were recorded. Figure 7 is the spectrum of the smoke from the ordinary mosquito-repellent incense and that dipped in the Mn (or Pb) solution and the high-purity Mn (or Pb). From the comparison diagram, the spectral lines of Mn (or Pb) in the spectrum of sample dipped in the solution can be accurately identified. Figure 7(a) shows six characteristic lines of Mn (257.62 nm, 259.38 nm, 260.65 nm, 403.01 nm, 403.24 nm and 403.35 nm), while Fig. 7(b) shows three characteristic lines of Pb (363.91 nm, 368.28 nm and 405.73 nm). As shown in Fig. 7(a), the large peak near 397 nm is the spectral line of Ca II (396.77 nm), which is from the mosquito-repellent incense. And the peak height of it changes from the ordinary smoke to the smoke containing element Mn. It could be explained by the proposal that the addition of new substance may lead to the self-absorption phenomenon.
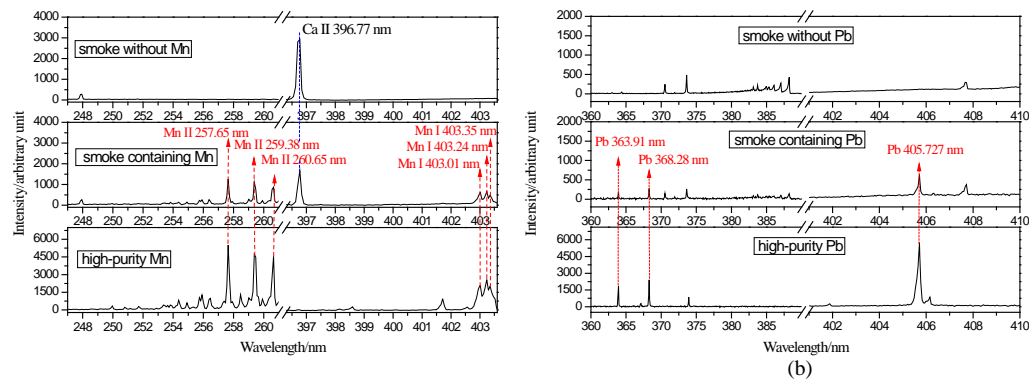
Fig. 7. The spectrum of two kinds of smoke and high-purity Mn (a), and the spectrum of two kinds of smoke and high-purity Pb (b).

Two solutions with different concentrations of manganese were prepared, as well as lead solutions. The three spectral lines of Mn that distributed around 403 nm and the three lines of Pb at 363.91 nm, 368.28 nm and 405.73 nm were selected for further analysis, because they have stronger intensity and are less disturbed by other elements. After the data process, it can be found in Fig. 8 that the relative intensity is proportional to the concentration of manganese and lead, which demonstrates it hopeful to have a quantitative analysis of the heavy metals in the atmosphere with LIBS technique.
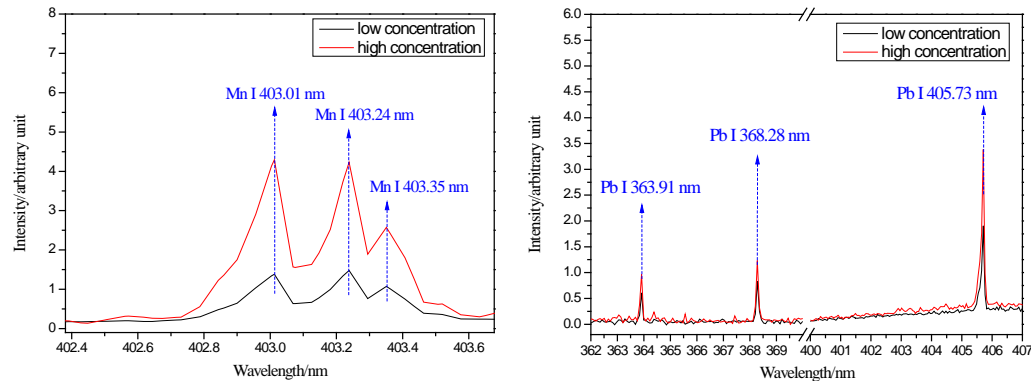

Fig. 8. The relative intensity of the characteristic spectral lines of Mn (a) and Pb (b) in the smoke.

4. Conclusion

In the experiment, LIBS technique was used for real-time detections of the ambient air, human breathing and smoke from burning mosquito-repellent incense. The characteristic peaks of nitrogen, oxygen and hydrogen (H_α) were observed, which are consistent with our knowledge of the air composition. There are some additional spectral lines being found in the spectrum of human breathing, such as the C I, H_β line and the CN molecular bands. However, the line of H_β has a weak intensity and probably because there is less water vapor in human breathing. It is supposed that CO_2 molecule may react with N_2 molecule to form CN. And the change of relative intensity of the element N can also be considered as an evidence to support the deduction. It is inferred that the carbon of the CN is likely to come from the CO_2 generating from the human breathing and the smoke with higher concentration. The smoke from burning mosquito-repellent incense was detected in situ with LIBS technique, and some metal elements have been found in the spectrum, such as Mg, Fe, Ca, Ti, Sr and Cr, which may cause pollution to the atmosphere. In addition, molecular bands of CN were also

recognized in the spectrum of smoke, and vibrational temperature of CN molecule in human breathing and smoke can be estimated to be 8200 K and 7900 K respectively, and the rotational temperature to be 7600 K and 7000 K. In order to simulate heavy metal pollution in the atmosphere, the mosquito-repellent incense was dipped into the solutions containing Mn and Pb element respectively to have a semiquantitative analysis. The results demonstrate it is promising to have a real-time detection and quantitative analysis on air pollution with LIBS. Further work on quantitative analysis is being in progress and could be expected.

References

1. J. C. Chow, "Health effects of fine particulate air pollution: lines that connect," J. Air Waste Manag. Assoc. **56**(6), 707–708 (2006).
2. J. T. Jørgensen, M. S. Johansen, L. Ravnskjær, K. K. Andersen, E. V. Bräuner, S. Loft, M. Ketzel, T. Becker, J. Brandt, O. Hertel, and Z. J. Andersen, "Long-term exposure to ambient air pollution and incidence of brain tumours: The Danish Nurse Cohort," Neurotoxicology **55**, 122–130 (2016).
3. A. Beal, F. de Almeida, C. A. B. Moreira, I. M. Santos, S. M. M. Curti, L. D. Martins, and C. R. T. Tarley, "A new analytical method for lead determination in atmospheric particulate matter by a combination of ultrasound-assisted extraction and supramolecular solvent preconcentration," Anal. Methods **10**(30), 3745–3753 (2018).
4. A. Cincinelli and A. Katsoyiannis, "Atmospheric pollution in city centres and urban environments. The impact of scientific, regulatory and industrial progress," Sci. Total Environ. **579**, 1057–1058 (2017).
5. C. M. González, C. D. Gómez, N. Y. Rojas, H. Acevedo, and B. H. Aristizábal, "Relative impact of on-road vehicular and point-source industrial emissions of air pollutants in a medium-sized Andean city," Atmos. Environ. **152**, 279–289 (2017).
6. S. Wang, A. Salamova, R. A. Hites, and M. Venier, "Spatial and Seasonal Distributions of Current Use Pesticides (CUPs) in the Atmospheric Particulate Phase in the Great Lakes Region," Environ. Sci. Technol. **52**(11), 6177–6186 (2018).
7. Y. Guan, G. Chen, Z. Cheng, B. Yan, and L. Hou, "Air pollutant emissions from straw open burning: A case study in Tianjin," Atmos. Environ. **171**, 155–164 (2017).
8. M. Kumar, R. K. Singh, V. Murari, A. K. Singh, R. S. Singh, and T. Banerjee, "Fireworks induced particle pollution: A spatio-temporal analysis," Atmos. Res. **180**, 78–91 (2016).
9. Q. Yu and Y. Z. Zhou, "High level of Mn in brain is a risk for Alzheimer disease," Sheng Li Xue Bao **70**(2), 193–200 (2018).
10. X. Lu, X. Xu, Y. Zhang, Y. Zhang, C. Wang, and X. Huo, "Elevated inflammatory Lp-PLA2 and IL-6 link e-waste Pb toxicity to cardiovascular risk factors in preschool children," Environ. Pollut. **234**, 601–609 (2018).
11. J. C. Chow, J. G. Watson, J. J. Shah, C. S. Kiang, C. Loh, M. Lev-On, J. M. Lents, M. J. Molina, and L. T. Molina, "Megacities and atmospheric pollution," J. Air Waste Manag. Assoc. **54**(10), 1226–1235 (2004).
12. C. G. Lilian, R. William, M. Robert, R. H. R. Carlos, D. C. Ricardo, C. G. Ana, D. Irma, F. L. Maricela, A. F. Mariana, S. Anna, C. A. Michael, T. J. Ricardo, and S. A. James, "Brain Inflammation and Alzheimer's-Like Pathology in Individuals Exposed to Severe Air Pollution," Circulation **32**(6), 650–658 (2015).
13. Q. Zhang, X. Jiang, D. Tong, S. J. Davis, H. Zhao, G. Geng, T. Feng, B. Zheng, Z. Lu, D. G. Streets, R. Ni, M. Brauer, A. van Donkelaar, R. V. Martin, H. Huo, Z. Liu, D. Pan, H. Kan, Y. Yan, J. Lin, K. He, and D. Guan, "Transboundary health impacts of transported global air pollution and international trade," Nature **543**(7647), 705–709 (2017).
14. T. S. Lin and F. M. Shen, "Trace metals in mosquito coil smoke," Bull. Environ. Contam. Toxicol. **74**(1), 184–189 (2005).
15. J. Vyhnanovský, J. Kratzer, O. Benada, T. Matoušek, Z. Mester, R. E. Sturgeon, J. Dědina, and S. Musil, "Diethyldithiocarbamate enhanced chemical generation of volatile palladium species, their characterization by AAS, ICP-MS, TEM and DART-MS and proposed mechanism of action," Anal. Chim. Acta **1005**, 16–26 (2018).
16. L. Nagli, M. Gaft, I. Gornushkin, and R. Glaus, "Stimulated emission and lasing in laser-induced plasma plume," Opt. Commun. **378**, 41–48 (2016).
17. A. Mansoori, B. Roshanzadeh, M. Khalaji, and S. H. Tavassoli, "Quantitative analysis of cement powder by laser induced breakdown spectroscopy," Opt. Lasers Eng. **49**(3), 318–323 (2011).
18. J. J. Choi, S. J. Choi, and J. J. Yoh, "Standoff Detection of Geological Samples of Metal, Rock, and Soil at Low Pressures Using Laser-Induced Breakdown Spectroscopy," Appl. Spectrosc. **70**(9), 1411–1419 (2016).

19. C. Aragón and J. A. Aguilera, "Direct analysis of aluminum alloys by CSigma laser-induced breakdown spectroscopy," Anal. Chim. Acta **1009**, 12–19 (2018).
20. I. Rehan, K. Rehan, S. Sultana, and R. Muhammad, "Laser Induced Breakdown Spectroscopy for Comparative Quantitative Analysis of Betel Leaves from Pakistan," Guangpuxue Yu Guangpu Fenxi **38**(10), 3295–3302 (2018).
21. S. Pagnotta, M. Lezzerini, B. Campanella, G. Gallello, E. Grifoni, S. Legnaioli, G. Lorenzetti, F. Poggialini, S. Raneri, A. Safi, and V. Palleschi, "Fast quantitative elemental mapping of highly inhomogeneous materials by micro-Laser-Induced Breakdown Spectroscopy," Spectrochim. Acta B At. Spectrosc. **146**, 9–15 (2018).
22. Y. Jia, N. J. Zhao, L. Fang, M. J. Fang, D. S. Meng, G. F. Yin, J. G. Liu, and W. Q. Liu, "Online calibration of laser-induced breakdown spectroscopy for detection of heavy metals in water," Plasma Sci. Technol. **20**(9), 131–136 (2018).
23. National Institute of Standards and Technology, "NIST Chemistry WebBook, SRD69," [retrieved 28.February 2019], http://webbook.nist.gov/chemistry/form-ser/
24. S. J. Mousavi, M. H. Farsani, S. M. R. Darbani, N. Asadorian, M. Soltanolkotabi, and A. E. Majd, "Identification of atomic lines and molecular bands of benzene and carbon disulfide liquids by using LIBS," Appl. Opt. **54**(7), 1713–1720 (2015).
25. G. P. Christian, "Atomic and molecular emissions in laser-induced breakdown spectroscopy," Spectrochim. Acta B At. Spectrosc. **79–80**, 4–16 (2013).
26. A. Fernández-Bravo, T. Delgado, P. Lucena, and J. J. Laserna, "Vibrational emission analysis of the CN molecules in laser-induced breakdown spectroscopy of organic compounds," Spectrochim. Acta B At. Spectrosc. **89**, 77–83 (2013).
27. A. Kushwaha and R. K. Thareja, "Dynamics of laser-ablated carbon plasma: formation of C2 and CN," Appl. Opt. **47**(31), G65–G71 (2008).
28. M. Cohen-Solal, "Strontium overload and toxicity: impact on renal osteodystrophy," Nephrol. Dial. Transplant. **17**(2 Suppl 2), 30–34 (2002).
29. R. Khlifi, P. Olmedo, F. Gil, B. Hammami, A. Chakroun, A. Rebai, and A. Hamza-Chaffai, "Arsenic, cadmium, chromium and nickel in cancerous and healthy tissues from patients with head and neck cancer," Sci. Total Environ. **452-453**, 58–67 (2013).
30. C. Wang, J. Ji, Z. Yang, and L. Chen, "The contamination and transfer of potentially toxic elements and their relations with iron, vanadium and titanium in the soil-rice system from Suzhou region, China," Environ. Earth Sci. **68**(1), 13–21 (2013).
31. G. Asimellis, S. Hamilton, A. Giannoudakos, and M. Kompitsas, "Controlled inert gas environment for enhanced chlorine and fluorine detection in the visible and near-infrared by laser-induced breakdown spectroscopy," Spectrochim. Acta B At. Spectrosc. **60**(7-8), 1132–1139 (2005).
32. M. Tran, Q. Sun, B. W. Smith, and J. D. Winefordner, "Determination of F, Cl, and Br in Solid Organic Compounds by Laser-Induced Plasma Spectroscopy," Appl. Spectrosc. **55**(6), 739–744 (2001).
33. J. Luque and D. R. Crosley, "LIFBASE: database and spectral simulation program (Version 1.5)," SRI Int. Rep. M **99**, 099 (1999).